Application of the Shell/3D Modeling Technique for the Analysis of Skin-Stiffener Debond Specimens

Ronald Krueger, T. Kevin O'Brien***

*ICASE

**U.S. Army Research Laboratory, Vehicle Technology Directorate

NASA Langley Research Center, Hampton, Virginia

Pierre J. Minguet

The Boeing Company, Philadelphia, Pennsylvania

ABSTRACT

The application of a shell/3D modeling technique for the simulation of skin/stringer debond in a specimen subjected to three-point bending is demonstrated. The global structure was modeled with shell elements. A local three-dimensional model, extending to about three specimen thicknesses on either side of the delamination front was used to capture the details of the damaged section. Computed total strain energy release rates and mixed-mode ratios obtained from shell/3D simulations were in good agreement with results obtained from full solid models. The good correlations of the results demonstrated the effectiveness of the shell/3D modeling technique for the investigation of skin/stiffener separation due to delamination in the adherents.

Keywords: delamination, skin/stringer debonding, finite element analysis, fracture mechanics

INTRODUCTION

Many composite components in aerospace structures are made of flat or curved panels with co-cured or adhesively-bonded frames and stiffeners. Testing of thin gage stiffened panels designed for pressurized aircraft or post-buckled rotorcraft fuselage applications has shown that bond failure at the tip of the frame flange is a very likely and important failure mode. Comparatively simple specimens consisting of a stringer flange bonded onto a skin were developed for investigating this mode of failure. The failure that initiates at the tip of the flange in these specimens is identical to the failure observed in the full-scale panels and the frame pull-off specimens. A consistent step-wise approach has been developed, which uses experiments to detect the failure mechanism, computational stress analysis to determine the location of first matrix cracking and computational fracture mechanics to investigate the potential for delamination growth [1].

In Proceedings of the American Society for Composites 17th Technical Conference, Purdue University, October 2002, CRC Press LLC, ISBN 0-8493-1501-8.

During previous studies two-dimensional finite element models were used for analysis to keep modeling and computational times remains affordable, especially if many different configurations have to be analyzed during the initial design phase [1, 2]. Results from a recent study where energy release rates from two-dimensional analyses were compared with data from full three-dimensional simulations indicated that plane stress and plane strain models yield upper- and lower-bound results. For more accurate predictions, however, a three-dimensional analysis is required [3]. For detailed modeling and analysis of the damage observed during the experiments, therefore, the shell/3D modeling technique appears to offer a great potential for saving modeling and computational effort because only a relatively small section in the vicinity of the delamination front needs to be modeled with solid elements. The technique combines the accuracy of the full three-dimensional solution with the computational efficiency of a shell finite element model, which has been demonstrated for various applications [4-6].

The objective of this study was to demonstrate the use of a shell/3D modeling technique for the simulation of skin/stringer debond in a specimen subjected to three-point bending as the technique will later be used for large, full-scale stringer stiffened panels. A local three-dimensional model, extending to about three specimen thicknesses on either side of the delamination front was used. Delaminations of various lengths were discretely modeled at the locations where delaminations were observed during the experiments. Mixed mode strain energy release rate distributions were computed across the width of the specimens using the virtual crack closure technique [7]. The results were compared to mixed mode strain energy release rates obtained from computations where the entire specimen had been modeled with solid elements [3].

BACKGROUND

The current study focused on skin-stiffener debonding resulting from buckling of a thin-gage skin composite fuselage structure as described in reference [2]. In that study, the specimens consisted of a bonded skin and flange assembly as shown in Figure 1(a). An IM7/8552 graphite/epoxy material system was used for both the skin and flange. The skin was made of prepreg tape with a measured average ply thickness of h =0.148 mm and had a [45/-45/0/-45/45/90/90/-45/45/0/45/-45] lay-up. The flange was made of a plain-weave fabric with a thickness of h =0.212 mm. The flange lay-up was $[45/0/45/0/45/0/45/0/45]_f$, where the subscript "f" denotes fabric, "0" represents a 0°-90° fabric ply and "45" represents a 0°-90° fabric ply rotated by 45°. The measured bondline thickness averaged 0.178mm. Specimens were 25.4-mm wide and 177.8-mm long.

Three-point bending tests were performed with a bottom support span of 101.6 mm as shown in Figure 1(b). The value of the damage onset load was averaged from four tests and determined to be Q =427.6 N with a coefficient of variation of 12.8%. The tests were terminated when the flange debonded from the skin. Damage was documented from photographs of the polished specimen edges at each of the four flange corners identified in Figure 1(a). Corners 1 and 4 and corners 2 and 3 showed identical damage patterns for both tests. The damage at corners 2 and 3, formed first and consisted of a matrix crack in the 45° skin surface ply and a delamination at the +45°/-45° interface as shown in Figure 2. This damage pattern was the focus of the current and related earlier analyses [2].

MODEL DESCRIPTION

The current study presents an intermediate step where three-dimensional models were created by extruding two-dimensional models across the width [2]. The fact that the delamination changed across the specimen width from a delamination running at the skin surface 45°/-45° layer interface (see Figure 2) to a delamination propagating in the bondline above, however, is still not accounted for in this model. Nevertheless, the three-dimensional model takes width effects into account and,

therefore, provides insight into the limitations of the use of the two-dimensional finite element models (FE) used earlier.

The deformed three-dimensional model of the specimen with load and boundary conditions is shown in Figure 3. The specimen was modeled using ABAQUS® solid twenty-noded hexahedral elements C3D20R with quadratic shape functions and a reduced integration scheme. This full three-dimensional model was used to generate the reference solutions to compare with results from the shell/3D simulations [3].

The deformed shell/3D model of the specimen is shown in Figure 4. The global section was modeled with ABAQUS® reduced integrated eight-noded quadrilateral shell elements S8R. The local three-dimensional model extended about three skin thicknesses on the side where the delamination originated from the matrix crack in the top 45° skin surface ply and extended to about three skin plus flange thicknesses beyond the maximum delamination length modeled. During the initial feasibility study the "rule of thumb" of extending the local three-dimensional model to about three specimen thicknesses on either side of the delamination had yielded good results [6]. The local three-dimensional section was almost identical to the equivalent segment of the full three-dimensional model shown in Figure 3, where a refined mesh was used in the critical area of the 45° skin ply where cracking was observed during the tests. Outside the refined area, the mesh was modified to prevent the three-dimensional model from becoming excessively large. The skin plies were grouped into four layered elements with 45/-45/0, -45/45/90, 90/-45/45 and 0/45/-45 stacks, thus taking advantage of the composite solid element option in ABAQUS® [8]. The fabric layers and the resin layer were grouped into five layered elements as shown in Figure 5. In the transition regions several plies were modeled by one element with material properties smeared using the rule of mixtures [9]. This procedure did not ensure the full contribution of the plies to the A, B, D, stiffness matrices. This method, however, appeared suitable for the small transition regions to enforce a reasonable model size. The transition from the global shell element model to the local three-dimensional model in the vicinity of the delamination front was accomplished by using multi-point constraint options given by ABAQUS® to enforce appropriate translations and rotations at the shell-solid interface [8]. Using the shell/3D approach the total number of degrees of freedoms could be reduced by more than 12% compared to the full three-dimensional model of the skin/stringer specimen. Nevertheless, for large built-up composite structures modeled using plate elements, the shell/3D modeling technique offers a great potential for reducing the model size, compared to a full three-dimensional model.

The Virtual Crack Closure Technique (VCCT) was used to calculate the mode I, II and III components of the strain energy release rates for the modeled delamination [7, 10]. For the entire investigation, the ABAQUS® geometric nonlinear analysis procedure was used. This was done in accordance with previous the studies which were used as reference solutions [3].

ANALYSIS RESULTS

Global Response

The deformed three-dimensional model and shell/3D model, including the boundary conditions, and the loads applied in the simulations are shown in Figures 3 and 4. A detail of the modeled delaminated region is shown in Figure 5. For short delamination lengths ($a < 1.0$ mm) crack opening mode I was apparent. For longer delaminations, the mode I response ceased and the surfaces near the free edge started to overlap [3]

The global response of the specimens was computed at the mean quasi-static damage onset load determined from experiments to examine whether the FE models, the boundary conditions, the loads and the material properties used in the model yielded reasonable results. The load-strain behavior computed from different FE models were compared to the corresponding experimental results. Strains

were averaged from computed nodal point values over a length corresponding to the dimensions of the strain gages shown in Figure 1(a) [3].

A comparison of measured strains at the surface of the flange (see Figure 1(a)) and computed results is shown in Figure 6. The strains calculated from the shell/3D model are in good agreement with the results from the full three-dimensional finite element model. The analysis results show a slightly stiffer response compared to the experimental results. This discrepancy may be due to using material properties from the literature in the FE simulations. For a consistent simulation, material data should be taken from the batch of material that was used to manufacture the specimens. For comparison, results from 2D analysis are included in the plot of Figure 6 [3]. Results from the plane-strain analysis indicated a stiffer behavior as expected. This is caused by the constraints inherent to the plane-strain model, particularly in the ±45° plies. The plane-stress model, which imposes the out-of-plane stresses to be zero and allows the displacement to be the free parameter exhibits a more compliant behavior as expected.

Fracture Mechanics Analysis

The objective of this study was to demonstrate the usefulness of the shell/3D modeling technique for the investigation of delamination onset from an initial crack. A fracture mechanics approach was used and during a series of nonlinear finite element analyses, strain energy release rates were computed at each delamination front location for the averaged damage onset load (Q =427.6 N) obtained from the experiments. A three-dimensional plot of the distribution of the total energy release rate, G_T, across the width of the specimen is shown in Figure 7. Values at the free edge (z=0.0 mm and z=25.4 mm) have been excluded from the plots as the model was not fine discretized enough to accurately capture the influence of the free edges on the distribution of the energy release rates. Along the length (x-coordinate) it was observed that G_T increases continuously, except for the zones near the free edges (z=0.0 mm and z=25.4 mm) where a sharp decrease is observed caused by the overlap of the interfaces after about 1 mm of delamination growth. Across the width (z-coordinate) the computed total energy release rate gradually increases with z before it drops off near the free edge (z=25.4 mm).

The total energy release rates along the centerline of the specimen (z=12.7 mm) obtained from three-dimensional and shell/3D analysis are plotted in Figure 8. The G_T versus x curves are continuously increasing, indicating unstable delamination growth. The values from the shell/3D analysis are within 6% of the results obtained from the full three-dimensional simulations. Improvements in results may be obtained by extending the section modeled with solid elements along the x-axis. The values from previous plain-strain and plane-stress analyses were included in Figure 8 for comparison [3]. All results follow the same trend, qualitatively. As before the values from 2D analysis form upper and lower bounds, except for very short delamination lengths.

The variation of mixed mode ratio G_S/G_T with delamination length is shown in Figure 9. Here G_S denotes the sum of the in-plane shearing components $G_{II}+G_{III}$, and G_T denotes the total energy release rate $G_I+G_{II}+G_{III}$, where G_I is the opening mode. For two-dimensional analyses, where G_{III}=0, this definition is equal to the commonly used definition of the mixed mode ratio, G_{II}/G_T. For three-dimensional analysis, which also yields results for the tearing mode, G_{III}, the modified definition of G_S is introduced.

For short delamination length the mixed mode ratio yields high shearing components, followed by a drop which is equivalent to an increase in opening mode I. For longer delaminations the shearing component remains constant. The values from shell/3D analyses are in good agreement with the results obtained from the full three-dimensional simulations. The values from previous plain-strain and plane-stress analyses were included in Figure 9 for comparison and follow the same trend [3]. The results from three-dimensional analysis in the center of the specimen (z=12.7 mm) show a higher shearing component compared to the results from two-dimensional analysis.

Computed total strain energy release rates and mixed mode ratios obtained form shell/3D simulations were in good agreement with results obtained from full solid models. The concurrence of the results demonstrated the effectiveness of the shell/3D modeling technique for the investigation of delamination onset from an initial crack. However, for the current configuration a reduction in computation time could not be achieved. Nevertheless, for large built-up composite structures modeled with plate elements, the shell/3D modeling technique offers a great potential for reducing the model size, compared to a full three-dimensional model.

CONCLUDING REMARKS

The application of the shell/3D modeling technique for the simulation of skin/stringer debond specimen subjected to three-point bending was demonstrated. The study extended the application of this technique beyond the simulation of simple specimens – such as DCB, ENF and SLB specimens – where the delamination is located between unidirectional plies in the mid-plane of the specimen. The global structure was modeled with shell elements. A three-dimensional model, extending to about three specimen thicknesses on either side of the delamination front was used locally. Delaminations of various lengths were discretely modeled at the locations where delaminations were observed during previous experiments.

Computed strains at the center of the flange were compared with results obtained from full three-dimensional finite element analysis and experimental data. Results from both analyses and experiment were in good agreement. Calculated total strain energy release rates and mixed mode ratios obtained form shell/3D simulations also were in good agreement with results obtained from full solid models. The concurrence of the results demonstrated the effectiveness of the shell/3D modeling technique for the investigation of delamination onset from an initial crack. For comparison results from plane-stress and plane-strain models provided flange strains, as well as energy release rates, which formed an upper and lower bound of the results obtained from full three-dimensional or shell/3D simulations.

The current study provided an additional verification step for the technique prior to its application to large, full-scale stringer stiffened panels because failure observed in the skin/stringer specimen is identical to the failure observed in the full-scale panels where the delamination is located between plies of different orientation. For large built-up composite structures modeled with plate elements, the shell/3D modeling technique offers a great potential for reducing the model size, compared to a full three-dimensional model, since only a relatively small section in the vicinity of the delamination front needs to be modeled with solid elements.

REFERENCES

1. Krueger, R., Cvitkovich, M. K., O'Brien, T. K., and Minguet, P. J., "Testing and Analysis of Composite Skin/Stringer Debonding Under Multi-Axial Loading," *J. Composite Materials*, Vol. 34, 2000, pp. 1263-1300.
2. Krueger, R., Paris, I. L., O'Brien, T. K., and Minguet, P. J., "Fatigue Life Methodology for Bonded Composite Skin/Stringer Configurations," *Journal of Composites Technology and Research*, Vol. 24, 2002, pp. 308-331.
3. Krueger, R. and Minguet, P. J., "Influence of 2D Finite Element Modeling Assumptions on Debonding Prediction For Composite Skin-Stiffener Specimens Subjected to Tension and Bending," NASA/CR-2002-211452, ICASE Report No. 2002-4, March 2002.
4. Dávila, C. G., "Solid-to-Shell Transition Elements for the Computation of Interlaminar Stresses," *Computing Systems in Engineering*, Vol. 5, 1994, pp. 193--202.

5. Wang, J. T., Dávila, C. G., Sleight, D. W., and Krishnamurthy, T., "Crown Panel Stiffener-Frame Intersection Structural Integrity Analyses," presented at the 5th NASA/DoD Conference on Advanced Composites Technology, Seattle, WA, 1994.
6. Krueger, R. and O'Brien, T. K., "A Shell/3D Modeling Technique for the Analysis of Delaminated Composite Laminates," *Composites Part A: Applied Science and Manufacturing*, Vol. 32, 2001, pp. 25-44.
7. Rybicki, E. F. and Kanninen, M. F., "A Finite Element Calculation of Stress Intensity Factors by a Modified Crack Closure Integral," *Eng. Fracture Mech.*, Vol. 9, 1977, pp. 931--938.
8. *ABAQUS/Standard - User's Manual - Version 5.6*, Vol. II: Hibbitt, Karlsson & Sorensen, Inc., 1996.
9. Tsai, S. W. and Hahn, H. T., *Introduction to Composite Materials*: Technomic Publishing Co., Inc., 1980.
10. Krueger, R., "The Virtual Crack Closure Technique: History, Approach and Applications," NASA/CR-2002-211628, ICASE Report No. 2002-10, May 2002.

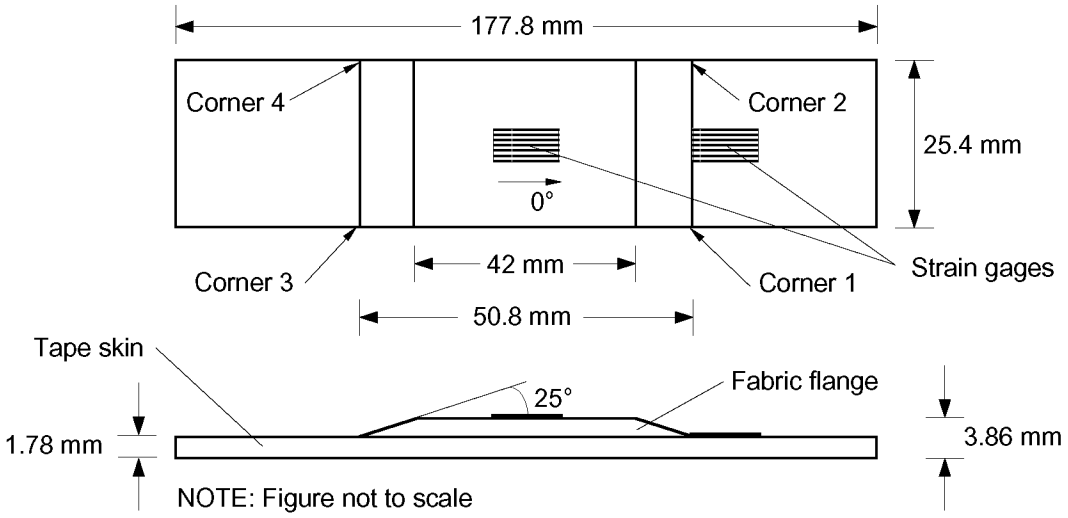

(a) Specimen configuration

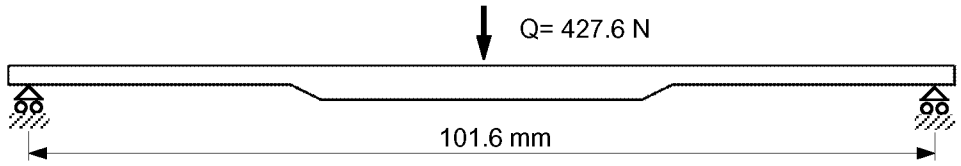

(b) Three-point bending

Figure 1 Specimen configuration and test set-up.

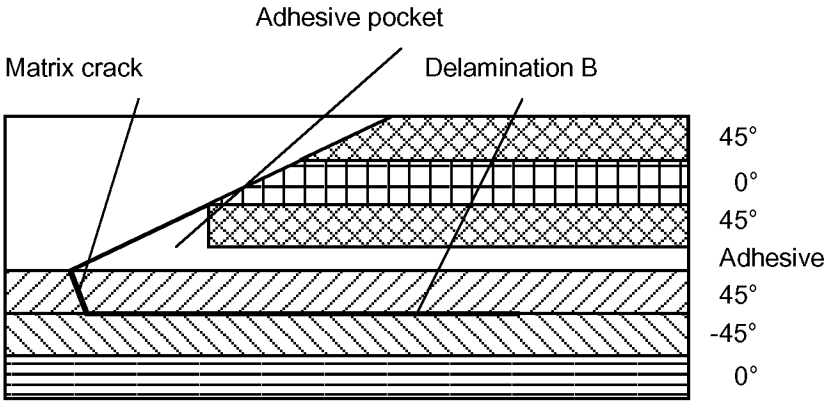

Figure 2 Typical damage patterns at specimen corners 2 and 3 [2,3].

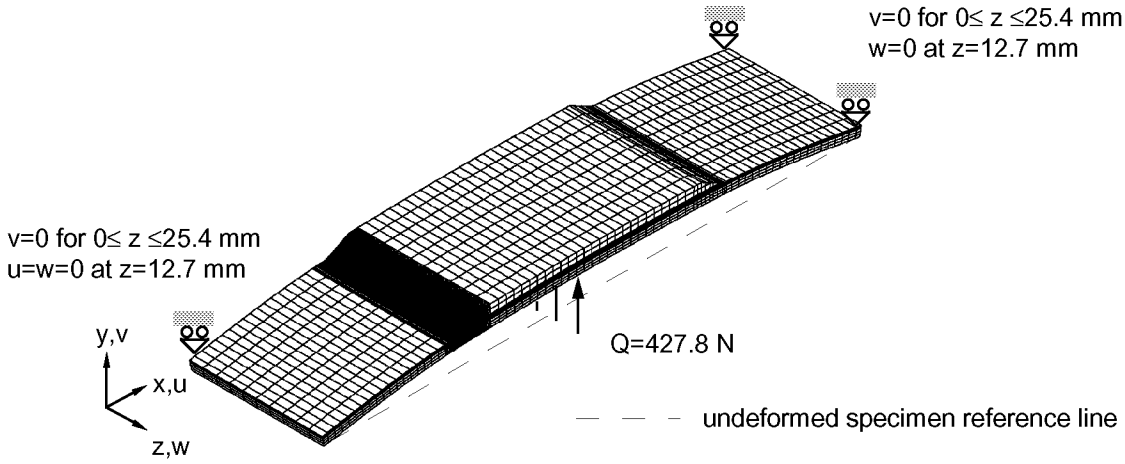

Figure 3 Deformed three-dimensional model with applied load and boundary conditions.

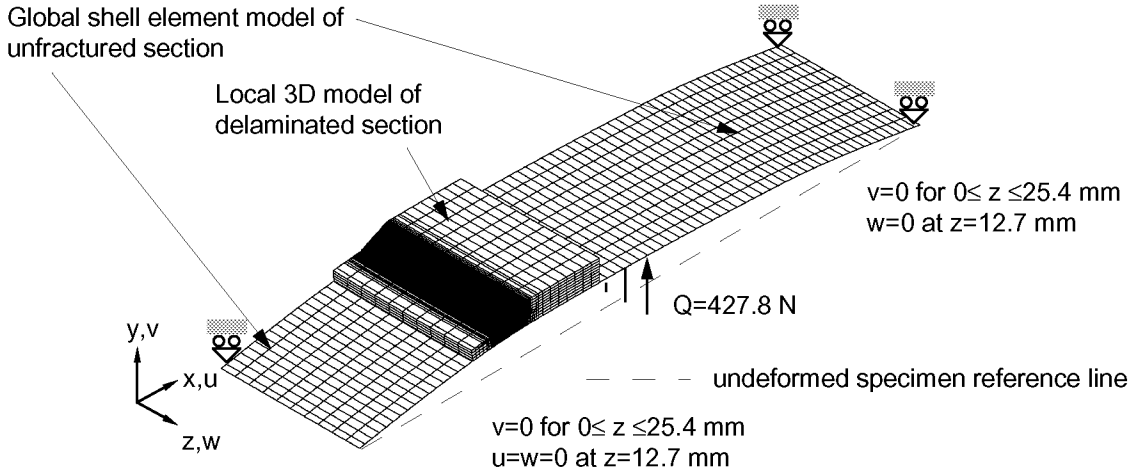

Figure 4 Deformed shell/3D model with applied load and boundary conditions.

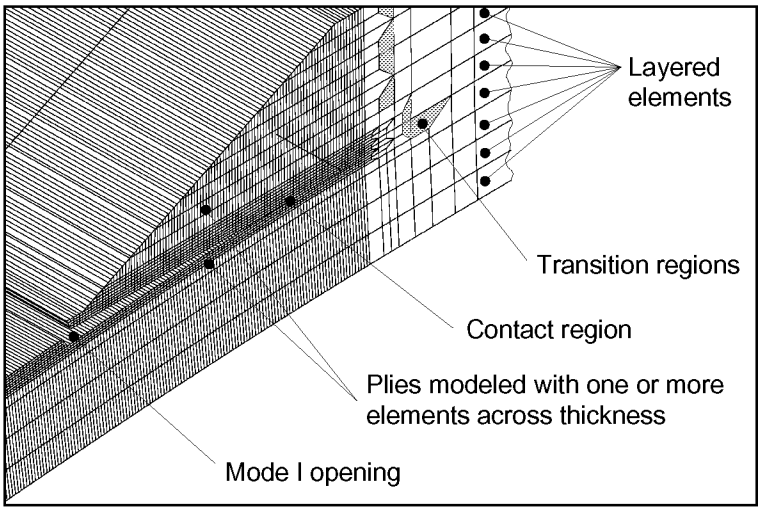

Figure 5 Detail for deformed model of the damaged specimen.

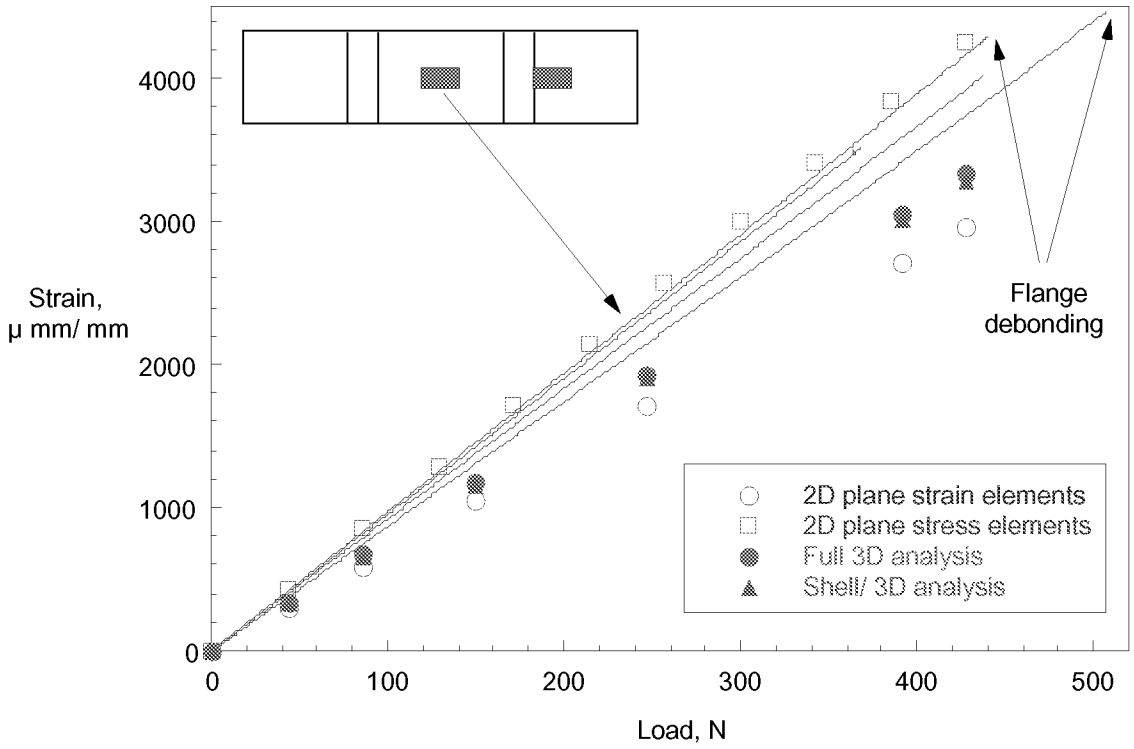

Figure 6.Flange strain-load plot.

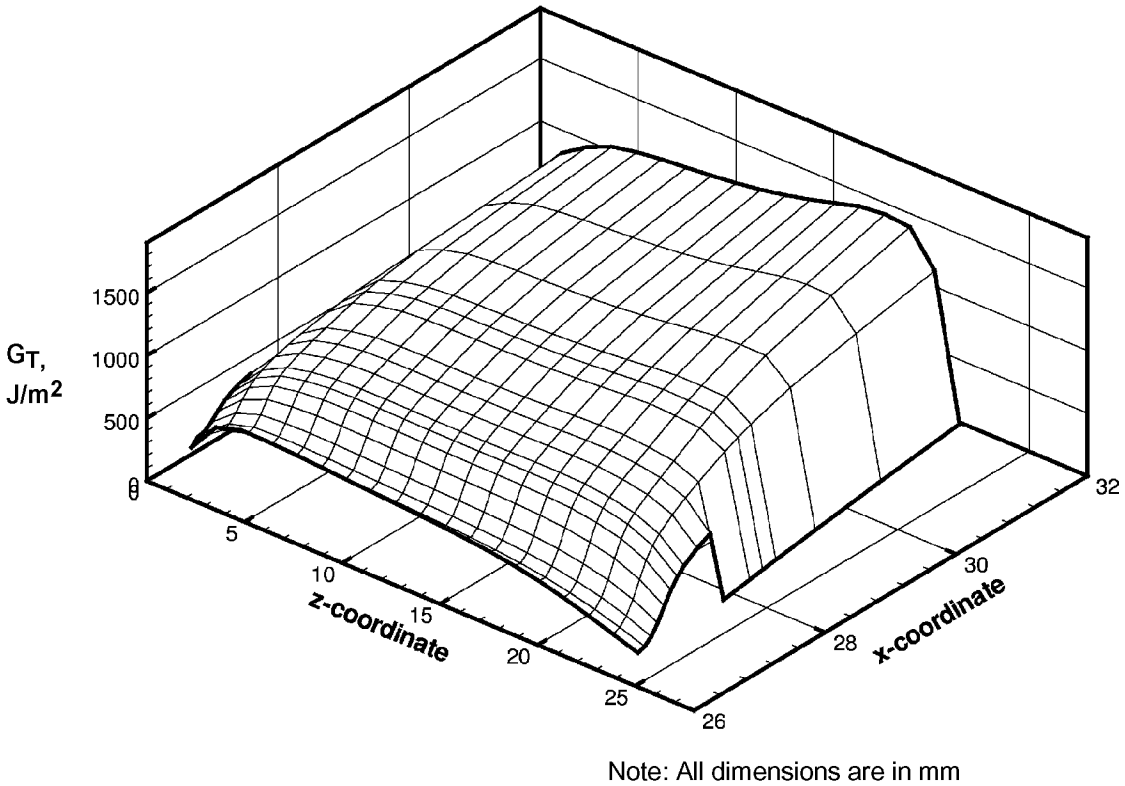

Figure 7.Computed total energy release rate distribution for damage onset load Q=427.6 N.

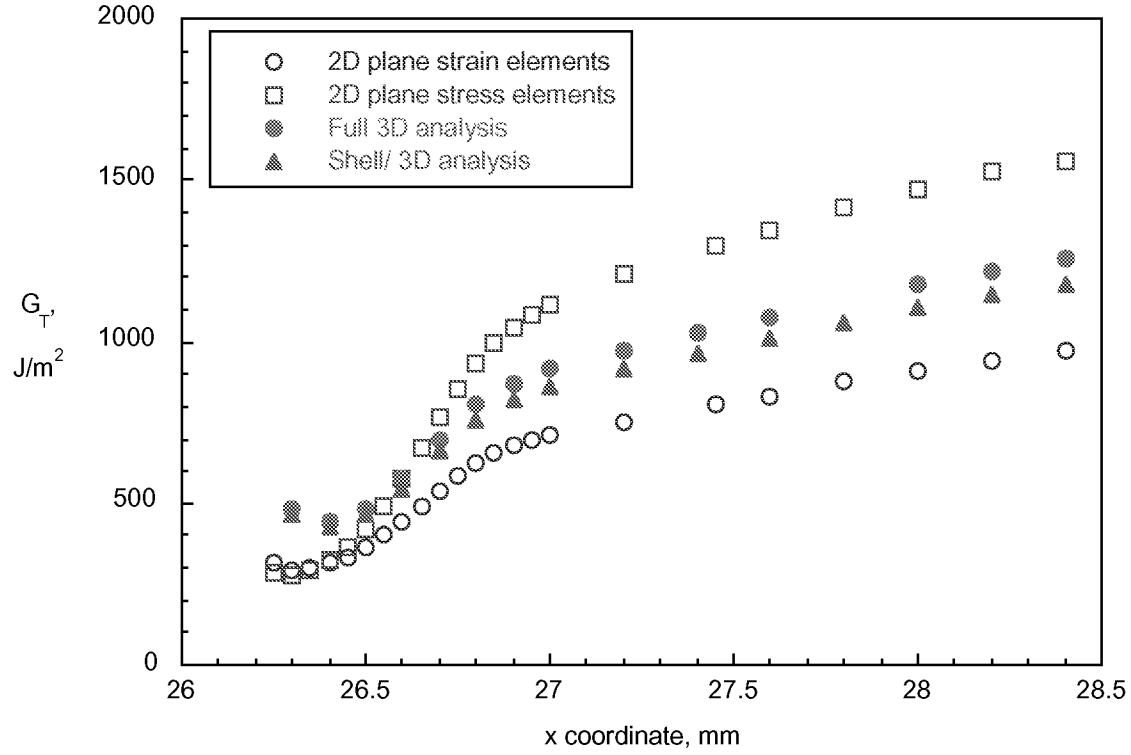

Figure 8 Computed total energy release rate at z=12.5 mm for damage onset load Q=427.6 N.

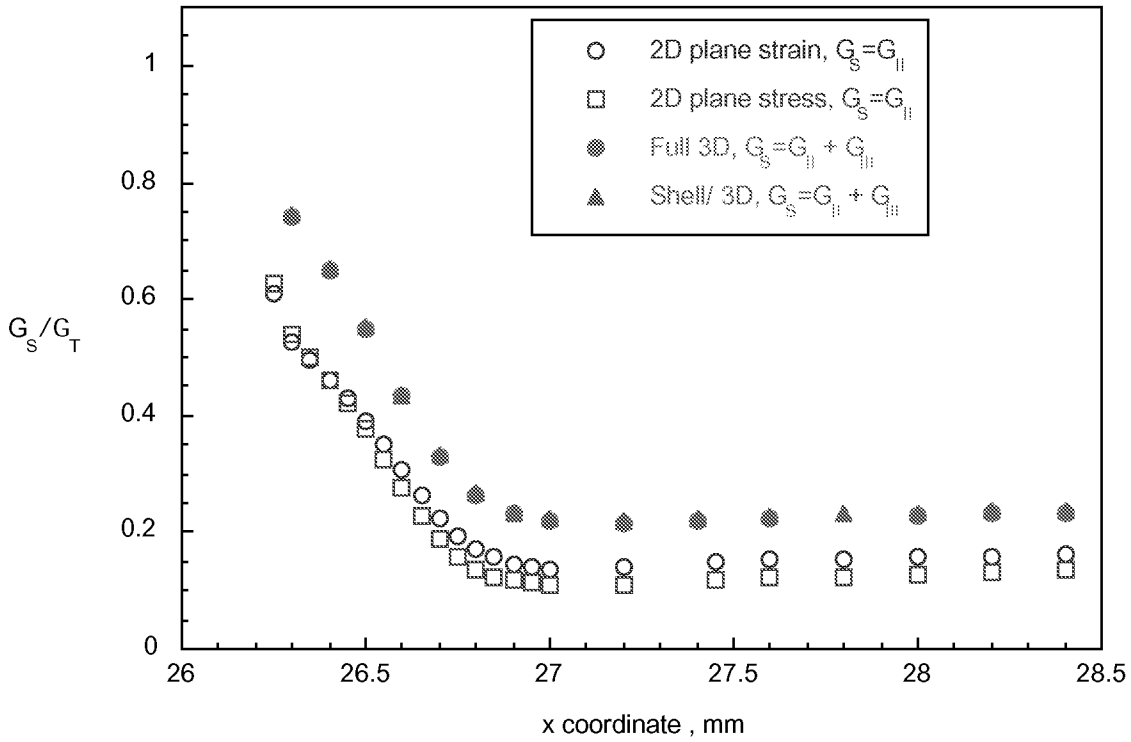

Figure 9 Computed mixed mode ratio G_S/G_T at z=12.5 mm for damage onset load Q=427.6 N.